https://doi.org/10.15407/scine20.01.074

GOLUBEK, A. V. (https://orcid.org/0000-0002-7764-6278)
Oles Honchar Dnipro National University,
72, Gagarina Ave., Dnipro, 49010, Ukraine.
+380 056 374 9807, prorektor_nr@dnu.dp.ua

CORRECTING MEASUREMENTS OF LAUNCH VEHICLE'S ANGULAR MOTION PARAMETERS OF A STRAPDOWN INERTIAL NAVIGATION SYSTEM WITH THE USE OF A CELESTIAL NAVIGATION SYSTEM

Introduction. *One of the tasks of developing strapdown inertial navigation systems with microelectromechanical sensors of launch vehicles is to ensure stringent requirements for the accuracy in determining the linear and angular motion with a guarantee of the successful completion of the satellite injection mission.*

Problem Statement. *The influence of a large range of random disturbances leads to degradation of the motion parameters of launch vehicle's strapdown inertial navigation system built with the use of microelectromechanical sensors. One of the ways to compensate for this degradation is the integrated use of inertial and celestial navigation systems.*

Purpose. *The purpose is to increase the satellite injection accuracy by launch vehicle using a strapdown inertial navigation system with microelectromechanical sensors due to a celestial navigation system with star tracker.*

Material and Methods. *Development of Kalman filter providing an integrated processing of measurements of angular motion parameters of a launch vehicle by a strapdown inertial navigation system and a star tracker. Statistical modelling of launch vehicle flight under the influence of various stochastic disturbances. Statistical processing of modelling results. Analysis of the proposed solution effectiveness.*

Results. *A workable mathematical model for correcting measurements of angular motion parameters of launch vehicle with the use of a Kalman filter has been developed. Its performance has been tested by the example of a launch vehicle injection into a sun synchronous orbit 700 km high with the use of a two-pulse injection scheme. It has been demonstrated that the proposed solution makes it possible to improve the accuracy of the angular orientation up to 90% and the satellite injection up to 5% in terms of altitude and orbit inclination.*

Conclusions. *The proposed development can be used to build navigation systems for advanced launch vehicles.*

Keywords: launch vehicle, strapdown inertial navigation system, celestial navigation system, microelectromechanical sensors, gyroscopes, star tracker, Kalman filter.

Citation: Golubek, A. V. (2024). Correcting Measurements of Launch Vehicle's Angular Motion Parameters of a Strapdown Inertial Navigation System with the Use of a Celestial Navigation System. *Sci. innov.*, 20(1), 74–86. https://doi.org/10.15407/scine20.01.074

The rapid development of microelectronics in recent decades has made it possible to provide the control systems of modern launch vehicle (LV) with high-performance on-board computers. This has allowed the application of an inertial navigation system based on the strapdown method in the motion control system. In comparison with the platform inertial navigation systems, these systems have advantages in terms of mass-dimensional characteristics and manufacturing cost. The use of linear and angular motion sensors built with the use of microelectromechanical (MEMS) technology enables achieving even greater miniaturization of the strapdown inertial navigation system (SINS). However, at the same time, their main disadvantage is low accuracy in determining the kinematic parameters of linear and angular LV motion. This leads to inexpediency of using inertial navigation in its pure form.

One of the methods for SINS improvement is its joint use with a global positioning system (GPS) [1—11]. Integrated processing of the measurements obtained by these positioning systems makes it possible to compensate for shortcomings of each of them and ensure high accuracy in determining the LV linear motion parameters. However, such architecture does not make it possible to compensate errors in determining the angular motion parameters, especially for launches lasting an hour or more.

At the same time, SINS knowledge of accurate data on the LV angular motion is necessary. On the one hand, satellite launch requestors can set requirements for the orientation and angular velocities of the satellite with respect to inertial space at the moment of separation from the LV. On the other hand, the process of LV injection into a predetermined orbit is carried out, in particular, by developing the program for direction of a vector of the propulsion system (PS) thrust with respect to inertial space. In practice, these limitations at the time of separation of the spacecraft from launch vehicle are about 1—5 degrees [12—15].

The LV angular orientation can be adjusted in flight through the integrated use of SINS and celestial navigation system (CNS). Such architecture has been considered in [16—24]. One of the CNS devices that enable determining the LV angular position with an accuracy of tens of angular seconds is the star tracker (ST). Its application makes it possible to adjust the accumulative drift of the angular orientation quaternion over the flight time, as well as partially compensate the instrumental errors in gyroscope measurement and errors in the initial alignment.

Therefore, the development of modern integrated navigation systems that enable determining the LV angular motion parameters in flight with a high accuracy for aerospace manufacturers of Ukraine is a crucial and important task.

The main areas of research close to the problem under consideration are as follows.

The integrated use of satellite-inertial navigation systems. Studies [7, 8] deal with the development of Kalman filter providing a complex processing of SINS and GPS navigation measurements in the case of non-Gaussian noise. Research [9] highlights a posteriori analysis of the navigation system of the light LV Vega using SINS and GPS. Research [10] deals with the development and modelling of a 6-dof mathematical model of the LV motion in the process of satellite injection into low Earth orbits. The authors of [11] have developed a mathematical model for the integrated processing of navigation measurements of SINS and GPS of a hypersonic vehicle using Kalman filter.

The complex use of stellar inertial navigation systems. Research [16] highlights developing a high-precision integrated navigation system for the SHEFEX-2 program. An architecture consisting of the integrated use of SINS, GPS, and CNS has been proposed. Research [17] deals with developing a new architecture for the integrated use of SINS and CNS to ensure the accuracy in determining the motion of an automatic cargo spacecraft. A model for integrated processing of navigation measurements has been synthesized. The cubature Kalman filter providing an integrated processing of navigation measurements of SINS, CNS, and GPS in the case of non-Gaussian noise

exposure has been developed in [18]. Research [19] highlights the problem of developing a mathematical model for the integrated use of SINS and CNS, which allows the estimate of gyroscopes drift and initial alignment of the satellite SINS. The problem of using stellar-inertial navigation as part of the motion control system of modern ballistic missiles has been solved in [20]. A new model for integrated processing of SINS and CNS measurements using the optimal Kalman filter for non-Gaussian noise has been proposed. Article [21] deals with improving the measurement accuracy of SINS accelerometers of modern vehicles using CNS. There has been proposed an improved method for the integrated processing of navigation measurements based on indirect measurement of star refraction traceable to horizon and providing an improvement in the positioning accuracy up to 90%. Research [22] deals with developing a new method of nonlinear filtration for integrating measurements of inertial navigation and celestial navigation systems using the cubature Kalman filter in the navigation system of a hypersonic vehicle. The proposed method makes it possible to eliminate the uncertainty of the dynamic model of inertial measurements and determine the damping coefficient using Mahalanobis distance theory. The problem of integrated processing of SINS, GPS, and CNS measurements using the quadrature Kalman filter has been considered in [23]. Article [24] deals with the development of a mathematical model for the integrated processing of measurements of SINS, GPS, and CNS of the LV using the extended Kalman filter. The proposed model makes it possible to partially compensate the errors in the initial alignment, sensitive axis setting, instrumental errors in the sensors, and method errors in gravity force calculation.

As for Ukraine, the following research areas close to the issue under consideration should be noted. A detailed analysis of the influence of SINS errors on the accuracy in light LV injection into typical near-Earth orbits has been carried out [6]. The list of determining disturbing factors, as well as the distribution parameters of the accuracy in the satellite injection and the deviations of the propellant load mass at the moment of separation of the satellite from the LV have been determined. Monograph [25] considers the methodology for assessing the accuracy in the injection of satellites by modern LV.

A priori and a posteriori accuracy of missiles developed by *Pivdenne* State Design Office. The accuracy in injection of the LV into near-Earth orbits with SINS using MEMS and GPS [26, 27] has been carried studied. The peculiarities of the influence of various errors on the accuracy in light LV injection into an equatorial orbit have been studied [28]. Studies [29, 30] deal with a priori estimation of the accuracy in ultralight LV injection into orbits with different inclinations. The list of determining disturbing factors and the limit deviations of the osculating parameters of the satellite orbit at the moment of separation from the LV have been revealed.

Based on the analysis of available achievements and publications, it follows that the problems of the accuracy of spacecraft injection by LV using SINS with MEMS sensors and CNS with ST in Ukraine still remain unsolved.

Let us consider the problem of correcting the LV angular motion according to the data of SINS gyroscopic instruments using CNS with the help of ST.

To solve it, the following is required:

- to synthesize a mathematical model for correcting measurements of angular motion parameters of SINS of the LV using CNS and Kalman filter;
- to simulate the satellite injection accuracy by the proposed model on the example of a problem of LV injection into a sun synchronous orbit using a two-pulse injection scheme;
- to carry out a comparative analysis of the accuracy in LV injection without CNS correction.

Let us introduce the following assumptions:

- LV is a variable-mass solid body moving under the influence of thrust force, the gravitation force of the Earth, and the aerodynamic drag force of the Earth's atmosphere;
- Earth's atmosphere — GOST 4401-81 and GOST 25645.115-84;

- the gravitational potential of the Earth takes into account the influence of the second, third, and fourth zonal harmonics;
- LV stabilization system is ideal;
- the impact of stochastic disturbances of SINS, GPS, CNS, PS characteristics, mass characteristics, and aerodynamic characteristics (ADC) is taken into account.

NAVIGATION MEASUREMENT CORRECTION MODEL

As is well known, the determining errors affecting the accuracy in determining the LV angular position with respect to the inertial space are the drift errors in the gyroscopes and the initial alignment of the SINS. Let's represent the error in measuring the LV angular position in the form of the following differential equation:

$$\Delta\dot{\Lambda}_S = \frac{1}{2}\left(\Lambda_L \circ \Delta\Omega_G + \Delta\Lambda_I \circ \Omega_L\right), \qquad (1)$$

where $\Delta\Lambda_S$ is an error quaternion in determining the LV orientation according to the SINS data; Λ_L is a quaternion of LV orientation; $\Delta\Omega_G$ is an error quaternion in measuring angular velocity by gyroscopes; $\Delta\Lambda_I$ is an error quaternion of SINS initial alignment; Ω_L is a quaternion of the angular velocity of the LV rotation around mass centre (MC).

Let us project (1) on the axis of the LV reference frame (LVRF):

$$\Delta\lambda_{S0} = -\frac{1}{2}\left(\lambda_{LX}\Delta\omega_{GX} + \lambda_{LY}\Delta\omega_{GY} + \lambda_{LZ}\Delta\omega_{GZ} + \right.$$
$$\left. + \Delta\lambda_{IX}\omega_{LX} + \Delta\lambda_{IY}\omega_{LY} + \Delta\lambda_{IZ}\omega_{LZ}\right), \qquad (2)$$

$$\Delta\lambda_{SX} = \frac{1}{2}\left(\lambda_{L0}\Delta\omega_{GX} + \lambda_{LY}\Delta\omega_{GZ} - \right.$$
$$\left. - \lambda_{LZ}\Delta\omega_{GY} + \Delta\lambda_{I0}\omega_{LX} + \Delta\lambda_{IY}\omega_{LZ} - \Delta\lambda_{IZ}\omega_{LY}\right), \qquad (3)$$

$$\Delta\lambda_{SY} = \frac{1}{2}\left(\lambda_{L0}\Delta\omega_{GY} - \lambda_{LX}\Delta\omega_{GZ} + \lambda_{LZ}\Delta\omega_{GX} + \right.$$
$$\left. + \Delta\lambda_{I0}\omega_{LY} - \Delta\lambda_{IX}\omega_{LZ} + \Delta\lambda_{IZ}\omega_{LX}\right), \qquad (4)$$

$$\Delta\lambda_{SZ} = \frac{1}{2}\left(\lambda_{L0}\Delta\omega_{GZ} + \lambda_{LX}\Delta\omega_{GY} - \lambda_{LY}\Delta\omega_{GX} + \right.$$
$$\left. + \Delta\lambda_{I0}\omega_{LZ} + \Delta\lambda_{IX}\omega_{LY} - \Delta\lambda_{IY}\omega_{LX}\right), \qquad (5)$$

where $\Delta\lambda_{S0}$, $\Delta\lambda_{SX}$, $\Delta\lambda_{SY}$, $\Delta\lambda_{SZ}$ are the elements of error quaternion in determining the orientation of the SINS LV; λ_{L0}, λ_{LX}, λ_{LY}, λ_{LZ} are the quaternion elements of LV orientation; $\Delta\omega_{GX}$, $\Delta\omega_{GY}$, $\Delta\omega_{GZ}$ are the projections of error vector for measuring the angular velocity of the LV rotation around MC by gyroscopes on the axis of the LV reference frame; $\Delta\lambda_{I0}$, $\Delta\lambda_{IX}$, $\Delta\lambda_{IY}$, $\Delta\lambda_{IZ}$ are the elements of an error quaternion of the SINS initial alignment; ω_{LX}, ω_{LY}, ω_{LZ} are the projections of a vector of the angular velocity of the LV rotation around MC on the axis of the LV reference frame.

The navigation information is integrated with the help of optimal predictor-corrector discrete-time Kalman filter [1—6, 31]. In this regard, let us define some vectors and matrices.

Based on (1)—(5), let us form a priori error vector $x(k, k)$ and fundamental matrix $F(k + 1, k)$ in the block form:

$$x(k, k) = [\Delta\lambda_{S0}\ \Delta\lambda_{SX}\ \Delta\lambda_{SY}\ \Delta\lambda_{SZ}$$
$$\Delta\omega_{GX}\ \Delta\omega_{GY}\ \Delta\omega_{GZ}\ \Delta\lambda_{I0}\ \Delta\lambda_{IX}\ \Delta\lambda_{IY}\ \Delta\lambda_{IZ}]^T, \qquad (6)$$

$$F(k+1, k) = \begin{pmatrix} E_4 & L & \Omega \\ O_{34} & E_3 & O_{34} \\ O_{44} & O_{43} & E_4 \end{pmatrix}, \qquad (7)$$

$$L = \begin{pmatrix} -\frac{1}{2}\lambda_{LX}\Delta t & -\frac{1}{2}\lambda_{LY}\Delta t & -\frac{1}{2}\lambda_{LZ}\Delta t \\ \frac{1}{2}\lambda_{L0}\Delta t & -\frac{1}{2}\lambda_{LZ}\Delta t & \frac{1}{2}\lambda_{LY}\Delta t \\ \frac{1}{2}\lambda_{LZ}\Delta t & \frac{1}{2}\lambda_{L0}\Delta t & -\frac{1}{2}\lambda_{LX}\Delta t \\ -\frac{1}{2}\lambda_{LY}\Delta t & \frac{1}{2}\lambda_{LX}\Delta t & \frac{1}{2}\lambda_{L0}\Delta t \end{pmatrix}, \qquad (8)$$

$$\Omega = \begin{pmatrix} 0 & -\frac{1}{2}\omega_{LX}\Delta t & -\frac{1}{2}\omega_{LY}\Delta t & -\frac{1}{2}\omega_{LZ}\Delta t \\ \frac{1}{2}\omega_{LX}\Delta t & 0 & \frac{1}{2}\omega_{LZ}\Delta t & -\frac{1}{2}\omega_{LY}\Delta t \\ \frac{1}{2}\omega_{LY}\Delta t & -\frac{1}{2}\omega_{LZ}\Delta t & 0 & \frac{1}{2}\omega_{LX}\Delta t \\ \frac{1}{2}\omega_{LZ}\Delta t & \frac{1}{2}\omega_{LY}\Delta t & -\frac{1}{2}\omega_{LX}\Delta t & 0 \end{pmatrix}, \qquad (9)$$

where E_3 and E_4 are the identity matrices 3 × 3 and 4 × 4, respectively; O_{34}, O_{43} and O_{44} are the zero matrices 3 × 4, 4 × 3, and 4 × 4, respectively.

Let us define the perturbation matrix $G(k+1, k)$ in the block form:

$$G(k+1,k) = \begin{pmatrix} L\frac{\Delta t}{2} \\ O_{33} \\ O_{43} \end{pmatrix}, \quad (10)$$

where O_{33} is the zero matrix 3 × 3.

Vector $z(k+1)$ and matrix $H(k+1)$ of measurement are predetermined by the following ratio:

$$z(k+1) = [\lambda_{S0} - \lambda^S_{S0}\lambda_{SX} - \lambda^S_{SX}\lambda_{SY} - \lambda^S_{SY}\lambda_{SZ} - \lambda^S_{SZ}]^T, \quad (11)$$

$$H(k+1) = (E_4\ O_{43}\ O_{44}), \quad (12)$$

where λ_{S0}, λ_{SX}, λ_{SY}, λ_{SZ} are the quaternion elements of the LV orientation according to SINS data; λ^S_{S0}, λ^S_{SX}, λ^S_{SY}, λ^S_{SZ} are the quaternion elements of the LV orientation according to ST data.

Let us find the noise covariance matrix from the following equation:

$$Q(k) = M_{S\leftarrow G}\begin{pmatrix} D_{GX} & 0 & 0 \\ 0 & D_{GY} & 0 \\ 0 & 0 & D_{GZ} \end{pmatrix} M_{G\leftarrow S}, \quad (13)$$

where D_{GX}, D_{GY}, D_{GZ} are the gyroscope drift dispersions; $M_{S\leftarrow G}$ и $M_{G\leftarrow S}$ are the transition matrices from the coordinate system related to the gyroscope sensitive axes, to the LV reference frame, and its inverse.

Let us define a posteriori error vector $x(k+1, k+1)$ from the following ratio:

$$H(k+1,k+1) = F(k+1,k)\,x(k,k) + K(k+1)[z(k+1) - H(k+1)\,F(k+1,k)\,x(k,k)], \quad (14)$$

$$K(k+1) = P(k+1,k)\,H(k+1)^T$$

$$P(k+1,k) = F(k+1,k)\,P(k,k)\,F(k+1,k)^T + G(k+1,k)\,Q(k)\,G(k+1,k)^T, \quad (15)$$

$$[H(k+1)\,P(k+1,k)\,H(k+1)^T + R(k)]^{-1}, \quad (16)$$

where $P(k, k)$ is the error measurement covariance matrix; $P(k+1, k)$ is the a priori error estimation covariance matrix; $K(k+1)$ is the Kalman gain matrix; $R(k)$ is the measurement covariance matrix determined by recalculating the angular accuracy in determining the ST orientation into the orientation quaternion with further statistical information processing.

Ratio (6)—(10) shall be supplemented with an equation determining a posteriori error estimation covariance matrix $P(k+1, k+1)$. It is used as an error measurement covariance matrix at the next operating cycle of Kalman filter.

$$P(k+1,k+1) = [E_{11} - K(k+1), H(k+1)]\,P(k+1,k), \quad (17)$$

where E_{11} is the identity matrix 11 × 11.

Further, the navigation information is adjusted with the use of the a posteriori error vector:

$$\lambda_{S0} = \lambda_{S0} - x(k+1,k+1)_1, \quad (18)$$

$$\lambda_{SX} = \lambda_{SX} - x(k+1,k+1)_2, \quad (19)$$

$$\lambda_{SY} = \lambda_{SY} - x(k+1,k+1)_3, \quad (20)$$

$$\lambda_{SZ} = \lambda_{SZ} - x(k+1,k+1)_4, \quad (21)$$

$$\begin{bmatrix} \omega_{GX} \\ \omega_{GY} \\ \omega_{GZ} \end{bmatrix} = \begin{bmatrix} \omega_{GX} \\ \omega_{GY} \\ \omega_{GZ} \end{bmatrix} - M_{G\leftarrow S}\begin{bmatrix} x(k+1,k+1)_5 \\ x(k+1,k+1)_6 \\ x(k+1,k+1)_7 \end{bmatrix}, \quad (22)$$

$$\Delta\tilde{\varphi}_I = -2x(k+1,k+1)_9, \quad (23)$$

$$\Delta\tilde{\psi}_I = -2x(k+1,k+1)_{10}, \quad (24)$$

$$\Delta\tilde{\vartheta}_I = -2x(k+1,k+1)_{11}, \quad (25)$$

where ω_{GX}, ω_{GY}, ω_{GZ} are the LV angular velocities measured by gyroscopes; $\Delta\tilde{\varphi}_I$, $\Delta\tilde{\psi}_I$, $\Delta\tilde{\vartheta}_I$ are the estimated initial alignment errors in roll, yaw, and pitch channels.

SIMULATION OF SATELLITE INJECTION ACCURACY

The disturbances involved are as follows:

1. SINS:

- the accelerometer errors: bias on run, bias run-run, bias error over broadband random vibration (BRV), axis misalignment;
- the gyroscope errors: bias on run, bias run-run, angular random walk, bias error over BRV, axis misalignment;

◆ other errors: method error of the initial alignment, quaternion drift.

2. The random errors in GPS measurement.

3. The random errors in ST measurement.

4. The errors in PS: thrust, mass flow rate, target section of jet pipe.

5. The errors in the mass-inertial and centring characteristics: stage's dry mass, filled stage propellant mass, payload fairing mass, satellite mass.

6. The errors in ADC: aerodynamic stage coefficients, stage midsection surface.

7. The errors in the atmospheric parameters.

The proposed model for integrating navigation information has been analysed by the example of a three-stages liquid light LV with the characteristics given in [32]. The satellite injection into a sun-synchronous orbit 700 km high is considered with the use of a two-pulse flight scheme described in detail in [6]. The errors in the characteristics of PS and ADC are given in [32], the errors in the SINS and GPS are assumed in accordance with [5, 6], the mass errors are considered in [32]. In order to simulate the LV motion, a stochastic, nonlinear discrete, adaptive motion model given in [6] has been adopted. It has the following vector form:

$$\dot{\bar{V}} = \dot{\bar{W}} + \bar{g}, \tag{26}$$

$$\dot{\bar{R}} = \bar{V}, \tag{27}$$

$$\dot{\Lambda} = \frac{1}{2}\Lambda \circ \Omega, \tag{28}$$

$$\dot{m} = -\dot{m}_{PS}, \tag{29}$$

$$\dot{\bar{V}}^* = \dot{\bar{W}}^* + \bar{g}^*, \tag{30}$$

$$\dot{\bar{R}}^* = \bar{V}^*, \tag{31}$$

$$\dot{\Lambda}^* = \frac{1}{2}\Lambda^* \circ \Omega^*, \tag{32}$$

$$\bar{g} = f_g(\bar{R}), \tag{33}$$

$$\bar{g}^* = f_g(\bar{R}^*) \tag{34}$$

$$\dot{\bar{W}}^* = \dot{\bar{W}} + \Delta\dot{\bar{W}}, \tag{35}$$

$$\Omega^* = \Omega + \Delta\Omega, \tag{36}$$

$$\Omega = \frac{2}{\Delta t}\tilde{\Lambda}^* \circ \Lambda_{PR}, \tag{37}$$

$$\Lambda_{PR} = f_\Lambda(\bar{R}^*, \bar{V}^*, \Omega^*, \Lambda^*, t), \tag{38}$$

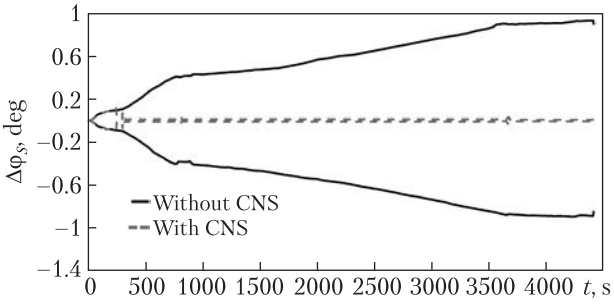

Fig. 1. Dependence of limit deviations of roll angle according to SINS data of implemented LV of the flight time

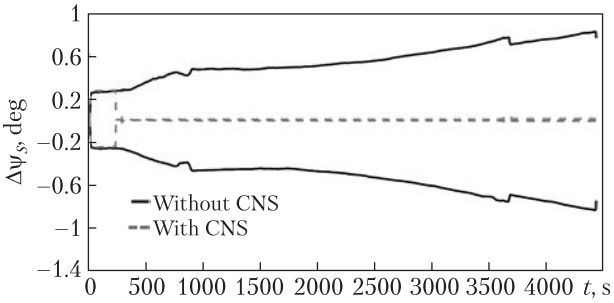

Fig. 2. Dependence of limit deviations of yaw angle according to SINS data of implemented LV of the flight time

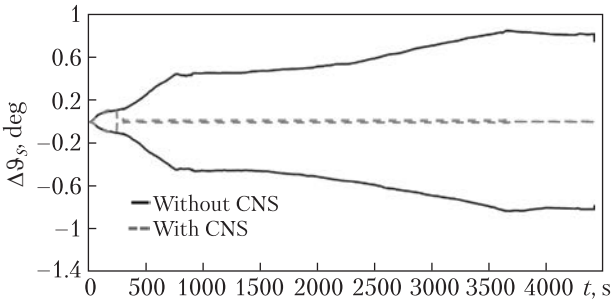

Fig. 3. Dependence of limit deviations of pitch angle according to SINS data of implemented LV of the flight time

$$\Delta\dot{\bar{W}} = f_W\left(\dot{\bar{W}}, \Lambda, \bar{\alpha}, \bar{\upsilon}\right), \tag{39}$$

$$\Delta\Omega = f_\Omega(\Omega, \bar{\gamma}, \bar{\upsilon}), \tag{40}$$

where $\bar{V}$ is the absolute velocity vector of LV MC; $\bar{W}$ is the apparent velocity vector of the LV MC; $\bar{g}$ is the Earth gravitational vector in the LV MC; $\bar{R}$ is the current position vector of the LV MC; Λ is the LV orientation quaternion with respect to inertial space; Ω is the angular velocity

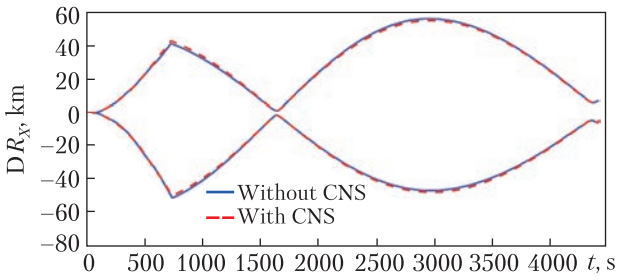

Fig. 4. Dependence of limit deviations of projection of the current position vector on the ILCF *X*-axis according to SINS data of implemented LV of the flight time

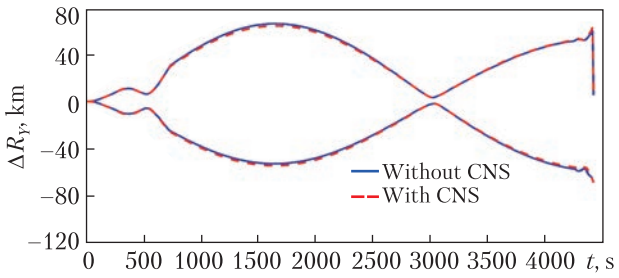

Fig. 5. Dependence of limit deviations of projection of the current position vector on the ILCF *Y*-axis according to SINS data of implemented LV of the flight time

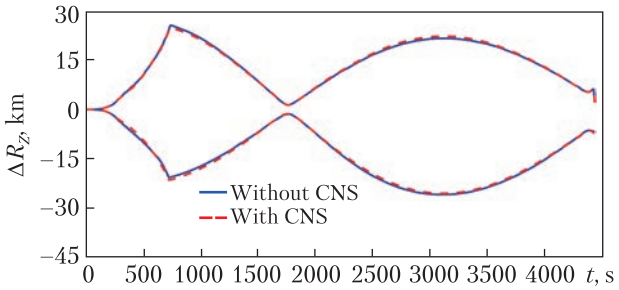

Fig. 6. Dependence of limit deviations of projection of the current position vector on the ILCF *Z*-axis of the according to SINS data of implemented LV of the flight time

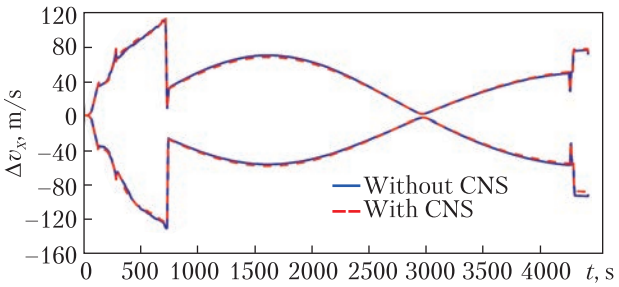

Fig. 7. Dependence of limit deviations of the projections of the absolute velocity vector on the ILCF *X*-axis according to SINS data of implemented LV of the flight time

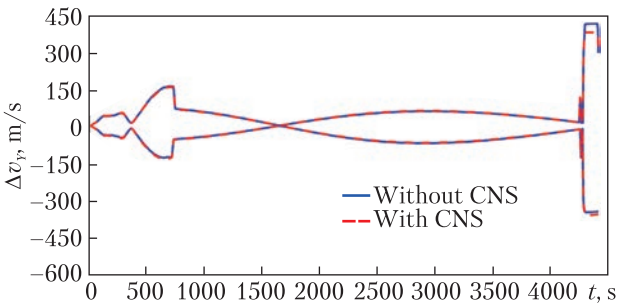

Fig. 8. Dependence of limit deviations of the projections of the absolute velocity vector on the ILCF *Y*-axis according to SINS data of implemented LV of the flight time

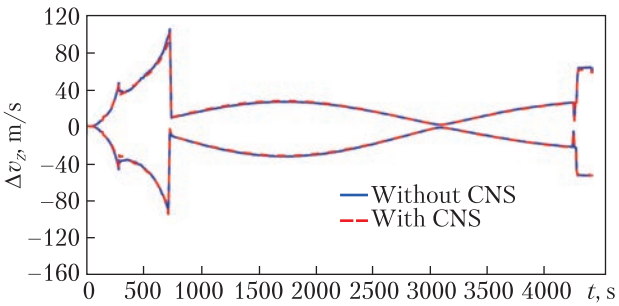

Fig. 9. Dependence of limit deviations of projection of the current position vector on the ILCF *Z*-axis according to SINS data of implemented LV of the flight time

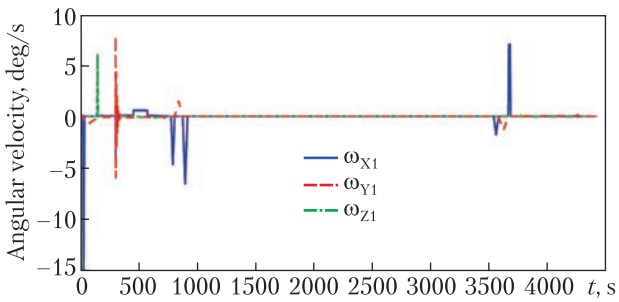

Fig. 10. Dependence of projections of the angular velocity vector on the LVRF axis of the flight time

quaternion of the LV rotation around MC; m is the LV current mass; $\dot{m}_{PS}$ is the PS mass fuel flow rate; $\bar{V}^*$ is the absolute velocity vector of the LV MC according to control system (CS) data; $\bar{W}^*$ is the apparent velocity vector of the LV MC according to CS data; $\bar{g}^*$ is the Earth gravitational vector in the LV MC according to CS data; $\bar{R}^*$ is

ISSN 2409-9066. Sci. innov. 2024. 20(1)

the current position vector of the LV MC according to CS data; Λ^* is the LV orientation quaternion with respect to inertial space according to CS data; Ω^* is the angular velocity quaternion of the LV rotation around CM according to CS data; $\Delta\bar{W}$ is the error vector of the apparent acceleration measurement by accelerometers; $\Delta\Omega$ is the error vector of the angular velocity measurement by gyroscopes; Λ_{PR} is the program quaternion calculated according to the LV guidance system data; t is the time; $\bar{\alpha}$ is the accelerometer error vector; $\bar{\upsilon}$ is the vector of methodological errors of the SINS initial alignment; $\bar{\gamma}$ is the gyroscope error vector; $f_g, f_\Lambda, f_W, f_\Omega$ are functions.

The detailed calculation of the right sides of differential (26)—(32) and algebraic (27)—(40) equations has been described in monograph [6].

The following devices are used for simulation:

- accelerometer — Model 1527 tactical-grade inertial MEMS surface mount accelerometer developed by Silicon Designs Inc [33];
- gyroscope — ER-MG2-100 high performance north seeking MEMS gyroscope developed by Ericco Inertial System [34];
- ST — PST3S-H2 Star Tracker developed by TY-Space Technology [35].

It is assumed that the ST is installed on the upper LV stage. The orientation of its axes coincides with the LV reference frame axes, the sighting axis coincides with the LV longitudinal axis. The device operation begins after LV escaping the Earth high-density atmosphere and ejecting the fairing (about 180 s of flight). In flight segments where the LV angular velocity vector modulus exceeds 1 deg/s, no ST measurements are made.

The injection process has been simulated by the Monte Carlo method for 10 thousand realizations of the initial conditions, given the considered perturbations. Two types of simulation have been carried out: without correction of SINS orientation data and with correction using the ST.

In order to assess the angular orientation accuracy in the roll, yaw and pitch channels, the extreme deviation value of 1 degree has been adopted.

COMPARATIVE ANALYSIS OF SATELLITE INJECTION ACCURACY

As a result of LV flight simulation with SINS and ST under predetermined conditions, trajectory tubes of linear and angular motion have been obtained, including:

- dependences of limit deviations (3σ) of orientation angles according to SINS data of implemented LV ($\Delta\varphi_S, \Delta\psi_S, \Delta\vartheta_S$) of the flight time ($t$) (Figs. 1—3);
- dependences of limit deviations of projections of the current position vector on the axis of the initial launch coordinate frame (ILCF) according to SINS data of implemented LV of the flight time ($\Delta R_{X_0}, \Delta R_{Y_0}, \Delta R_{Z_0}$) (Figs. 4—6);
- dependences of limit deviations of the projections of the absolute velocity vector on the ILCF axis according to SINS data of implemented LV of the flight time ($\Delta V_{X_0}, \Delta V_{Y_0}, \Delta V_{Z_0}$) (Figs. 7—9).
- dependence of projections of the angular velocity vector on the LVRF axis of the flight time is shown in Fig. 10.

According to the data obtained (Figs. 1—3), it can be concluded that for the considered flight pattern and the selected devices, the satellite angular orientation accuracy at the moment of separation from the LV is ensured (extreme deviation is less than 1 degree in the roll, yaw and pitch channels). But the safety factor is insignificant. Changing the flight mission, the initial simulation conditions, the flight pattern, the conditions for abstracting or refinement of characteristics of MEMS sensors based on the results of flight tests can lead to the output of the angular orientation parameters beyond the accepted ones. The LV angular orientation tube in the roll, yaw and pitch channels at the moment of satellite separation is narrowed by more than 90% due to the CNS use. In this case, the tubes of parameter deviations of linear motion change within the limits of up to 13%.

Let's consider the influence of CNS application on the accuracy of ensuring the osculating and kinematic parameters of the satellite orbit at the moment of separation from the LV. The parame-

Table 1. **Parameters of the Distribution of Deviations of the Osculating Orbit Parameters at the Moment of Satellite Separation from LV**

Parameter	Δα, m	Δe, 10^{-5}	Δi, deg	ΔΩ, deg	Δω, deg	Δu, deg
CNS excluded						
Mean	–1177	9.0	0.000	0.000	–0.741	–0.389
Standard deviation	1181	7.8	0.003	0.004	1.521	0.299
Minimum limit value	–6195	–7.7	–0.011	–0.012	–3.130	–0.974
Maximum limit value	1502	40.7	0.010	0.012	3.129	0.856
CNS included						
Mean	–1152	8.8	0.000	0.000	–1.070	–0.392
Standard deviation	1148	7.5	0.003	0.001	1.143	0.298
Minimum limit value	–6021	–8.1	–0.010	–0.004	–3.117	–0.993
Maximum limit value	1411	40.2	0.010	0.004	3.117	1.008

Table 2. **Parameters of the Distribution of Deviations of the Kinematic Orbit Parameters at the Moment of Satellite Separation from LV**

Parameter	ΔR_{X_0}, m	ΔR_{Y_0}, m	ΔR_{Z_0}, m	ΔV_{X_0}, m/s	ΔV_{Y_0}, m/s	ΔV_{Z_0}, m/s
CNS excluded						
Mean	10672	–36033	29828	–49.067	–3.671	12.571
Standard deviation	7888	27716	23034	37.780	2.755	9.585
Minimum limit value	–21598	–90254	–66397	–122.884	–9.565	–26.966
Maximum limit value	26546	79486	74685	108.730	7.004	31.674
CNS included						
Mean	10752	–36340	30085	–49.490	–3.707	12.680
Standard deviation	7973	28288	23528	38.584	2.735	9.730
Minimum limit value	–24911	–92320	–78687	–125.557	–9.529	–31.596
Maximum limit value	27011	95404	75687	129.767	7.983	32.228

Table 3. **Limit Deviations of Satellite Separation Time and Propellant Load Mass**

Parameter	Limit deviations (3σ)			
	CNS excluded		CNS included	
	min	max	min	max
Separation time, s	42.08	–19.04	94.72	–19.00
Propellant load mass, kg	318.523	–343.806	323.216	–331.132

ters of the distribution of deviations of the controlled osculating parameters are presented in Table 1, while the kinematic parameters are given in Table 2. The designations of the osculating parameters in Table 1: Δa is the semi-major axis deviation, Δe is the eccentricity deviation, Δi is the inclination deviation, $\Delta\Omega$ is the RAAN deviation, $\Delta\omega$ is the deviation of the perigee argument, Δu is the deviation of the latitude argument.

As can be seen from the data in Table 1, the CNS implementation slightly changes the distribution of deviations of the orbit osculating parameters. At the same time, the range of distribution of the semi-major axis, eccentricity, inclination, right ascension of ascending node, and argument of perigee latitude decreases by 3.4%, 0.2%, 4.8%, 66.7%, and 0.4%, respectively, the range of latitude argument increases by 9.3%.

As for deviations of kinematic parameters (Table 2), there is a decrease in the distribution range up to 11% in the projections of the current position vector of the ILCF axis and in the projections of the absolute velocity vector on the ILCF axis.

Let's consider the influence of CNS application on the deviation of the time of formation of the command to separate the satellite from the LV and the deviation of the propellant load mass (Table 3).

It follows from the data in Table 3 that due to the CNS use, the range of time distribution of the satellite separation from the LV increases by 86% (about 43 s), and the fuel component mass at the moment of separation from the LV decreases by 1.2% (about 8 kg).

CONCLUSIONS

As a result of the research, the problem of increasing spacecraft injection accuracy by LV using a SINS with MEMS sensors and a CNS with ST has been solved. The following results have been obtained.

1. A mathematical model for correcting the measurements of angular motion parameters of SINS of the LV with the use of CNS and Kalman filter has been developed.

2. The satellite injection accuracy has been simulated with the help of the proposed model by the example of LV injection into a sun synchronous orbit using a two-pulse injection scheme.

3. It has been shown that when using advanced MEMS sensors, the satellite angular orientation accuracy of 1 degree in the roll, yaw and pitch channels at the moment of separation from the LV is ensured. But changing the flight mission, the initial simulation conditions, the flight pattern, the conditions for abstracting or refining the characteristics of MEMS sensors based on the results of flight tests can lead to the output of the angular orientation parameters beyond the accepted ones.

4. The comparative analysis of the LV injection accuracy has been carried out with and without the use of CNS correction.

5. It has been demonstrated that the integrated use of SINS and CNS makes it possible to narrow the tube of LV angular orientation deviation in the roll, pitch, and yaw channels at the moment of satellite separation by 90%.

6. It has been shown that at the moment of satellite separation from the LV, the range of distribution of the semi-major axis, eccentricity, inclination, right ascension of ascending node, and argument of perigee latitude decreases by 3.4%, 0.2%, 4.8%, 66.7%, and 0.4%, respectively, while the range of latitude argument increases by 9.3%.

7. There has been reported a decrease in the distribution range of deviations of satellite kinematic parameters at the moment of separation from the LV up to 11% in the projections of the current position vector of the ILCF axis and in the projections of the absolute velocity vector on the ILCF axis.

8. It has been determined that the range of time distribution of the satellite separation from the LV increases by 86% (about 43 s), and the fuel component mass at the moment of separation from the LV decreases by 1.2% (about 8 kg).

The proposed mathematical model for correcting the measurements of angular motion parameters in an adapted form can be used as part of the software using SINS sensors of modern LV adjusted by CNS.

REFERENCES

1. Rogers, R. M. (2003). *Applied mathematics in integrated navigation systems*. Reston.
2. Titterton, D. H., Weston, J. L. (2004). *Strapdown inertial navigation technology.* London.
3. Farrell, J. A. (2008). *Aided navigation GPS with high rate sensors*. The McGraw-Hill Companies.
4. Groves, P. D. (2008). *Principles of GNSS, inertial, and multisensor integrated navigation systems*. Artech House.
5. Design of control systems for objects of rocket and cosmetic equipment. T. 1. Design of launch vehicle control systems. (2012). Eds. Yu. S. Alekseeva, Yu. M. Zlatkina, V. S. Krivtsova, A. S. Kulika, V. I. Chumachenko. Kharkiv (in Russian).
6. Golubek, A. V., Filippenko, I. M., Tatarevskii, K. E. (2019). A priori estimation of satellite's injection accuracy by modern launch vehicles with SINS: monograph. Dnipro [in Russian].
7. Zhao, C., Yang, Z., Cheng, X., Hu, J., Hou, X. (2022). SINS/GNSS integrated navigation system based on maximum versoria filter. *Chinese Journal of Aeronautics,* 35(8), 168–178. https://doi.org/10.1016/j.cja.2021.10.024.
8. Cánepa, V., Servidia, P., Giribet, J. (2022). Adaptive extended Kalman filter for integrated navigation in a satellite launch vehicle. *2022 IEEE Biennial Congress of Argentina (San Juan, Argentina*). 1–8. https://doi.org/10.1109/ARGENCON55245.2022.9939949.
9. Vandersteen, J., Bennani, S., Roux, C. (2017). Robust rocket navigation with sensor uncertainties: Vega launcher application. *Journal of Spacecraft and Rockets*, 55(1), 1—14. https://doi.org/10.2514/1.A33884.
10. Sreena, P. V., Thomas, T. (2017). Orbit injection error mitigation by time-differenced GPS carrier phase observables-aided inertial navigation. *AIAA Guidance, Navigation, and Control Conference* (*January 2017*).
11. Chen, K., Zhou, J., Shen, F.-Q., Sun, H.-Y., Fan, H. (2020). Hypersonic boost-glide vehicle strapdown inertial navigation system / global positioning system algorithm in a launch-centered earth-fixed frame. *Aerospace Science and Technology*, 98, 105679. https://doi.org/10.1016/j.ast.2020.105679.
12. Falcon user's guide. September 2021. URL: https://www.spacex.com/media/falcon-users-guide-2021-09.pdf (Last accessed: 24.05.2023).
13. Ariane 5 user's manual. Iss. 5, rev. 1. July 2011. URL: https://www.arianespace.com/wp-content/uploads/2015/09/Ariane5_users_manual_Issue5_July2011.pdf (Last accessed: 24.05.2023).
14. Cyclone-4 launch vehicle user's guide. Iss. 1. October 2010. URL: https://www.mach5lowdown.com/wp-content/uploads/PUG/Cyclone-4-users-guide-2010-10.pdf (Last accessed: 24.05.2023).
15. Cyclone-4M SLS ABBREVIATED USER'S GUIDE. Ver. 2. May 2019. URL: https://www.maritimelaunch.com/sites/default/files/UG_C4M%20abbreviated.pdf (Last accessed: 24.05.2023).
16. Vallverdú, D., Pou, C., Badenas, M., Diez, E. (2018). Application of a hybrid navigation system for an autonomous space air-launched vehicle. *ERTS* (*January 2018*). Toulouse, France.
17. Wang, D., Lv, H, An, X., Wu, J. (2018). A high-accuracy constrained SINS/CNS tight integrated navigation for high-orbit automated transfer vehicles. *Acta Astronautica*, 151, 614—625. https://doi.org/10.1016/j.actaastro.2018.07.015.
18. Wang, D., Lv, H., Wu, J. (2017). A novel SINS/CNS integrated navigation method using model constraints for ballistic vehicle applications. *The Journal of Navigation,* 70(6), 1415—1437. https://doi.org/10.1017/S0373463317000418.
19. Zhu, J., Wang, X., Li, H., Che, H., Li, Q. (2018). A high-accuracy SINS/CNS integrated navigation scheme based on overall optimal correction. *The Journal of Navigation*, 71(6), 1567—1588. https://doi.org/10.1017/S0373463318000346.
20. Hou, B., He, Z., Li, D., Zhou, H., Wang, J. (2018). Maximum correntropy unscented Kalman filter for ballistic missile navigation system based on SINS/CNS deeply integrated mode. *Sensors,* 18(6), 1724. https://doi.org/10.3390/s18061724.
21. Shi, C., Chen, X., Wang, J. (2023). A correcting accelerometer errors algorithm for SINS/CNS integrated system. *Advances in Guidance, Navigation and Control,* 845, 4651—4660. https://doi.org/10.1007/978-981-19-6613-2_451.
22. Gao, B., Li, W., Hu, G., Zhong, Y., Zhu, X. (2022). Mahalanobis distance-based fading cubature Kalman filter with augmented mechanism for hypersonic vehicle INS/CNS autonomous integration, *Chinese Journal of Aeronautics,* 35(5), 114—128. https://doi.org/10.1016/j.cja.2021.08.035.
23. Gao, B., Hu, G., Zhong, Y., Zhu, X. (2022). Distributed state fusion using sparse-grid quadrature filter with application to INS/CNS/GNSS integration. *IEEE Sensors Journal*, 22(4), 3430—3441. https://doi.org/10.1109/JSEN.2021.3139641.
24. Zhang, L., Yang, H., Zhang, S., Cai, H., Qian, S. (2014). Strapdown stellar-inertial guidance system for launch vehicle. *Aerospace Science and Technology,* 33(1), 122—134. https://doi.org/10.1016/j.ast.2014.01.007.
25. Novykov, O., Tikhonov, V., Litvinov, V. *Methods of analysis for launch vehicle injection accuracy:* monograph. Vilnius.
26. Degtyarev, A. V., Degtyarev, M. A., Davydenko, S. A., Makarov, A. L., Snegirev, M. G., Sirenko, V. N., Tikhonov, V. L., Shekhovtsov, V. S. (2015). On the feasible development of gimballess control systems for launch vehicles using GPS satellite navigation equipment. *Space Science and Technology*, 21(6), 3—12 [in Russian].

27. Chucha, Y., Tikhonov, V., Degtyareva, E., Sidorenko, S., Matviyenko, E., Lapko, A., Laylyuk, S. (2019). Performance evaluation of GINS built by MEMS technology, without and with the use of integration with SNS UE. *The 7-th International conference "Space technologies: present and future"* (21—24 May 2019, Dnipro). 132.
28. Golubek, A. V. (2020). A priori analysis of the injection accuracy of a launch vehicle into equatorial orbit. *Adaptive Systems of Automatic Control*, 2(37), 74—86.
29. Smyrnov, A. S., Golubek, A. V. (2021). Estimation of the influence of errors of the SINS constructed on MEMS components on the accuracy of positioning an ultra-light class rocket. *Aerospace Technic and Technology*, 5, 60—68. https://doi.org/10.32620/aktt.2021.5.08 [in Russian].
30. Smyrnov, A. S., Holubek, O. V. (2022). Impact analysis of MEMS-components errors of SINS on accuracy of satellite launch via ultralight launch vehicle. *Journal of Rocket-Space Technology*, 30(4), 57—65. https://doi.org/10.15421/452209 [in Ukrainian].
31. Lewis, F. L., Xie, L., Popa, D. (2008). *Optimal and robust estimation with an introduction to stochastic control theory*. CRC Press.
32. Igdalov, I. M., Kuchma, L. D., Poliakov, N. V., Sheptun, Yu. D. (2013). *Dynamic problems of rockets and spaces stages*: monograph. Dniepropetrovsk.
33. Model 1527 tactical-grade inertial MEMS surface mount accelerometer datasheet. Silicon Designs Inc. URL: https://www.silicondesigns.com/_files/ugd/ 3fcdcf_55ec5e50f1314ea485456990cb7983c5.pdf (Last accessed: 24.05.2023).
34. ER-MG2-100 North-Seeking MEMS Gyro datasheet. Ericco Inertial System. URL: https://www.ericcointernational.com/wp-content/uploads/2021/09/ER-MG2-100-North-Seeking-MEMS-Gyroscope_20220708100631.pdf (Last accessed: 24.05.2023).
35. Star Tracker. URL: https://satsearch.s3.eu-central-1.amazonaws.com/datasheets/satsearch_datasheet_3nmqtj_tyspace_star_tracker_sun_tracker_portfolio.pdf?X-Amz-Algorithm=AWS4-HMAC-SHA256&X-Amz-Credential=AKIAJLB7IRZ54RAMS36Q%2F20230224%2Feu-central-1%2Fs3%2Faws4_request&X-Amz-Date=20230224T144654Z&X-Amz-Expires=86400&X-Amz-Signature=11f419ff9cbffb608e24f9b0f3d5934538248fb82000deae41ae469b75770541&X-Amz-SignedHeaders=host. (Last accessed: 24.05.2023).

Received 26.03.2023
Revised 04.05.2023
Accepted 30.06.2023

О.В. Голубек (https://orcid.org/0000-0002-7764-6278)

Дніпровський національний університет імені Олеся Гончара,
просп. Гагаріна, 72, Дніпро, 49010, Україна,
+380 056 374 9807, prorektor_nr@dnu.dp.ua

КОРЕКЦІЯ ВИМІРЮВАНЬ ОБЕРТАЛЬНОГО РУХУ РАКЕТИ КОСМІЧНОГО ПРИЗНАЧЕНИЯ БЕЗПЛАТФОРМНОЇ ІНЕРЦІАЛЬНОЇ НАВІГАЦІЙНОЇ СИСТЕМИ З ВИКОРИСТАННЯМ АСТРОНАВІГАЦІЙНОЇ СИСТЕМИ

Вступ. Одним із завдань розробки безплатформних інерціальних навігаційних систем із мікроелектромеханічними сенсорами ракет космічного призначення є забезпечення жорстких вимог до точності визначення поступального й обертального руху, що гарантують вдале виконання місії виведення супутників.

Проблематика. Вплив широкого спектру випадкових збурень призводить до деградації параметрів руху безплатформної інерціальної навігаційної системи ракети космічного призначення, побудованої із застосуванням мікроелектромеханічних сенсорів. Одним із шляхів компенсації цієї деградації є комплексне застосування систем інерціальної навігації та астронавігації.

Мета. Підвищення точності виведення супутника ракетою космічного призначення з використанням безплатформної інерціальної навігаційної системи з мікроелектромеханічними сенсорами через застосування астронавігаційної системи із зірковим датчиком.

Матеріали й методи. Розробка фільтра Калмана, що забезпечує комплексну обробку вимірювань параметрів обертального руху ракети безплатформною інерціальною навігаційною системою і зірковим датчиком. Статистичне моделювання польоту ракети космічного призначення в умовах дії різноманітних стохастичних збурень. Статистична обробка результатів моделювання. Аналіз ефективності запропонованого рішення.

Результати. Розроблено працездатну математичну модель корекції вимірювань параметрів обертального руху ракети космічного призначення з використанням фільтра Калмана. Перевірено її працездатність на прикладі запуску ракети космічного призначення на сонячно-синхронну орбіту висотою 700 км з використанням двоімпульсної схеми виведення. Показано, що використання запропонованого рішення дозволяє підвищити точність визначення кутової орієнтації до 90 %, а також підвищити точність виведення супутника за висотою та нахиленням орбіти до 5 %.

Висновки. Запропоновану розробку можна застосувати для побудови навігаційних систем сучасних ракет космічного призначення.

Ключові слова: ракета космічного призначення, безплатформна інерціальна навігаційна система, мікроелектромеханічні сенсори, астронавігаційна система, зірковий датчик, фільтр Калмана.